Stoch Environ Res Risk Assess (2005) 19: 388–402
DOI 10.1007/s00477-005-0010-9

ORIGINAL PAPER

Richard Dawson · Jim Hall · Paul Sayers
Paul Bates · Corina Rosu

Sampling-based flood risk analysis for fluvial dike systems

Published online: 8 October 2005

Abstract A dike system of moderate size has a large number of potential system states, and the loading imposed on the system is inherently random. If the system should fail, in one of its many potential failure modes, the topography of UK floodplains is usually such that hydrodynamic modelling of flood inundation is required to generate realistic estimates of flood depth and hence damage. To do so for all possible failure states may require 1,000s of computationally expensive inundation simulations. A risk-based sampling technique is proposed in order to reduce the computational resources required to estimate flood risk. The approach is novel in that the loading and dike system states (obtained using a simplified reliability analysis) are sampled according to the contribution that a given region of the space of basic variables makes to risk. The methodology is demonstrated in a strategic flood risk assessment for the city of Burton-upon-Trent in the UK. 5,000 inundation model simulations were run although it was shown that the flood risk estimate converged adequately after approximately half this number. The case study demonstrates that, amongst other factors, risk is a complex function of loadings, dike resistance, floodplain topography and the spatial distribution of floodplain assets. The application of this approach allows flood risk managers to obtain an improved understanding of the flooding system, its vulnerabilities and the most efficient means of allocating resource to improve performance. It may also be used to test how the system may respond to future external perturbations.

Keywords Flood risk assessment · Reliability analysis · Monte Carlo · Infrastructure systems · Flood management

R. Dawson (✉) · J. Hall
School of Civil Engineering and Geosciences,
University of Newcastle-upon-Tyne, Cassie Building,
Newcastle-upon-Tyne, NE17RU UK
E-mail: richard.dawson@newcastle.ac.uk
Tel.: +44-191-2223660
Fax: +44-191-2226502
E-mail: jim.hall@newcastle.ac.uk

P. Sayers
HR Wallingford Ltd, Howbery Park, Wallingford,
Oxfordshire, OX108BA UK
E-mail: pbs@hrwallingford.co.uk

P. Bates
School of Geographical Sciences, Bristol University,
University Road, Bristol, BS81SS UK
E-mail: paul.bates@bris.ac.uk

C. Rosu
University "Politehnica" Timisoara,
2 Piata Victoriei, Timisoara, Romania
E-mail: ccnnrr@yahoo.com

Introduction

Approximately 8% of the land area of England (around 10,000 km^2) is at risk of flooding from rivers, tidal rivers and estuaries (NAO 2001). Floodplains are relatively densely developed, containing approximately 1 million residential and non-residential properties worth nearly £100 billion and over 1.5 million hectares of agricultural land worth approximately £5 billion (Halcrow et al. 2001). These assets are protected by some 33,000 km of dikes. However, serious flooding in 1998 and 2000 demonstrated the need for improved management of flood dikes (Bye and Horner 1998; Environment Agency 2001; ICE 2001).

Flood risk assessment provides a rational basis for the development of flood management policy, allocation of resources and monitoring the performance of flood management activities on local, regional and national scales (eg. USACE 1996; Moser 1997; NRC 2000; Vrijling 2001; Sayers et al. 2002; Hall et al. 2003a, b). The methodology presented in this paper forms part of a tiered approach to risk assessment under development in England and Wales (Hall et al. 2003b), of which a national scale risk assessment forms the broadest scale of assessment whilst the methodology described herein has been developed to support broad-scale (strategic)

management of dike systems. The method provides a snap-shot of flood risk at present or in a future scenario of floodplain development, climate change or dike geometry and condition.

Methods of reliability analysis have been classified into three levels (JCSS 1981). Traditional design uses level I methods, in which safety factors are imposed on the loading and resistance variables. For level II methods, the failure surface is approximated with a first or higher order Taylor series expansion around the point on the failure surface closest to the origin (often known as the 'design point'), after the joint probability density function (jpdf) describing the basic variables has been transformed into independent normally distributed variables. In level III methods, the integral of the jpdf that describes the basic variables is solved numerically. The research described in this paper is based on level III methods.

Considerable data and computational requirements have, until recently, meant flood risk assessment that incorporates reliability analysis of dike systems has not been possible at a broad scale. Complex infrastructure systems (such as dike systems) have a large number of possible system failure states. Each of these possible failure states may contribute towards the total flood risk associated with the system, yet for a large system the computational resources needed to calculate the contributions for all these states may be unavailable. This is further compounded by the complex topography of floodplains in the UK (and many other countries) for which significant computational time is required to model inundation in order to obtain realistic estimates of the impacts of flooding.

Reliability techniques (eg. Melchers 1999) focus on accurately estimating the probability of system failure as opposed to risk. However, the conditions resulting in the greatest probability of failure do not necessarily result in the greatest flood risk: a weak dike protecting scrubland may be likely to fail, but will contribute little towards flood risk, conversely failure of a strong dike defending a city may contribute greatly towards flood risk. The aim of this paper is to develop an efficient method for estimating risk, for which probabilities of system failure are a necessary but not sufficient requirement.

The research described in this paper is clearly related to recent work in the Netherlands analysing and optimising the risk associated with systems of dikes (Voortman et al. 2003). However, the complex topography of UK floodplains means that more emphasis on flood inundation modelling is required in order to generate realistic estimates of flood depth and hence damage. This differs from the approach of Voortman et al. (2003) where fairly simple assumptions of the depth of inundation could be made. Studies by Jonkman et al. (2003) and others have employed the more detailed hydrodynamic modelling similar to that used in this paper. However, this has been employed for a relatively small number of failure scenarios at the water level corresponding to the design point, whilst here we demonstrate that a more comprehensive sampling strategy is required to obtain accurate risk estimates for the UK river floodplain studied.

Following this introductory section the relevant principles of flood risk analysis for dike systems are introduced. Aspects of reliability theory for series systems are reviewed. We briefly introduce the hydrodynamic modelling methodology that has been used to simulate river and floodplain flows in the analysis. Next the steps in the flood risk assessment methodology are described, with particular reference to the numerical method. The example application to Burton-upon-Trent is presented before concluding with discussion of the benefits and limitations of the proposed approach.

Flood risk analysis for discrete systems under continuous loading

Flood risk is traditionally defined as the product of the probability of flooding and the consequential damage. Economic risk is often expressed in terms of an expected annual damage, EAD, (often referred to as the average annual damage). Measures of other risks have been proposed (eg. Jorissen and Stallen 1998; USACE 1999; Bedford and Cooke 2001; Tapsell et al. 2002; Jonkman et al. 2003) but are not considered here. Of interest in this paper are river floodplains protected by series systems of dikes. In a series system, failure of one or more components results in system failure, in this case defined as inundation of part or all of the floodplain. Each dike section $i = 1,..., n$ is considered to be a discrete system component. We wish to estimate a probability distribution of flood depths for specified locations or zones in the floodplain. Flooding may occur due to the overflowing of one or more dikes (i.e. the water level in the river at the dike exceeding the dike crest level), by breaching of one or more dikes (i.e. structural failure leading to removal of part or all of the dike cross-section) or by a combination thereof. Flooding due to overflowing and breaching are dealt with differently in the methodology because the two processes have quite different implications for the inundation modelling.

At sites with topography of any complexity it is necessary to use a hydrodynamic model to simulate floodplain inundation and estimate flood depths. The hydrodynamic modelling approach adopted here is discussed briefly below, but there are several widely available modelling packages that could be used for the task. If dikes are included as geometric features on the land surface then dike overflow is represented automatically in the hydrodynamic modelling. However, in the event of a dike breach the land surface boundary of the hydrodynamic model has to be modified to represent the breach. Thus overflow events are included in the hydrodynamic modelling, given a particular inflow hydrograph, so do not require explicit attention in the probabilistic calculations, though of course the consequences of flooding caused by overflow have to be

included in the risk calculation. On the other hand the probability of one or more breach events has to be calculated and the inundation modelling specifically run to estimate the impacts of these events. Breaching is assumed to be simultaneous for multiple dike failure combinations, eliminating the temporal component of breach sequencing from the analysis.

Suppose that the breaching of dike section i is represented by the event B_i. Thus the system state $\overline{B_1} \cap \overline{B_2} \cap \ldots \cap \overline{B_n}$ represents the condition in which none of the dike sections have breached, so from the structure point of view the system is completely safe. There are 2^n system states of which 2^n-1 are breached states. Depending on the water level in the river at each dike section (and we take this to be a deterministic function of the flow Q at the upstream boundary of the site) the water depth (which may be zero) and hence the flood damage at every point in the model domain can be calculated. Flood damage is taken as a deterministic function of flood depth.

The analysis method therefore deals with two uncertainties in the calculation of risk:

1. The flow Q in the river at the upstream boundary of the site. This uncertainty is represented by a probability density function $f(Q)$.
2. The resistance of each dike section i ($i=1,\ldots, n$) in the dike system to loading. This uncertainty is represented by a discrete probability distribution over the dike system states, conditional upon loading Q.

We require the joint probability distribution, which is continuous over the flow Q and discrete over the dike system states, S_j: $j=1,\ldots, 2^n$. Given a flow Q and a dike state S_j there is a damage function $D(Q,S_j)$, where the units of $D_{Q,\,j}$ are £ or some suitable currency. The total flood risk, in terms of EAD, is therefore given by:

$$R = \int_0^\infty \sum_{j=1}^{2^n} P(S_j|Q) f(Q) D(Q, S_j) \mathrm{d}Q, \qquad (1)$$

where by definition $\sum_{j=1}^{2^n} P(S_j|Q) = 1$ and $\int_0^\infty f(Q)\,\mathrm{d}Q = 1$.

Calculation of the function $D(Q,S_j)$ is computationally expensive as it involves hydrodynamic modelling. For a dike system of any complexity 2^n is a large number (n is likely to be 15–40 for a 10 km reach). Therefore, evaluation of Eq. 1 will in general be computationally expensive, possibly excessively so. To do so we make a number of simplifying assumptions and numerical approximations, which are now discussed.

Discrete flood dike systems reliability analysis

In analysis of the reliability dike system, divided into discrete sections, protecting a self-contained floodplain, we make two assumptions:

1. The resistance of each dike section of independent of other sections in the system, conditional upon the loading.
2. The dike resistance can be adequately described by a fragility function i.e. a conditional probability distribution of dike failure given loading. Justification for the first assumption is that the main source of dependency between discrete sections in a dike system originates from the loading. Meanwhile, the resistance of each section is assessed independently. The resistance of some dike sections, particularly those located near each other and sharing similar failure modes may not be completely independent–perhaps due to shared geotechnical conditions. However, Van Gelder and Vrijling (1998) suggest that these types of spatial correlation may tend to zero over 50–100 m which justifies the assumption of independence, conditional upon loading.

The fragility, $P(B_i|l)$, of a component i is the probability of the failure event B_i, conditional on a specific loading, l (Casciati and Faravelli 1991). A fragility curve (Fig. 1) provides a useful summary of the performance of a flood defence structure (Dawson and Hall 2002a, b). Fragility may be a function of several, not necessarily independent, loading variables $l_1,\ldots,l_q$. The (unconditional) breach probability of a dike section, $P(B_i)$, can be established by integrating the fragility function over the loading distributions:

$$P(B_i) = \int_0^\infty f(l_1, \ldots, l_q) P(B_i l_1, \ldots, lq) \mathrm{d}l_1, \ldots, l_q, \qquad (2)$$

where $f(l_1,\ldots, l_q)$ is a joint probability density over q non-negative loading variables and $P(B_i|l_1,\ldots, l_q)$ is the fragility function conditional on the loading(s). For a fluvial dike, the loading will generally be water level, W_i, at

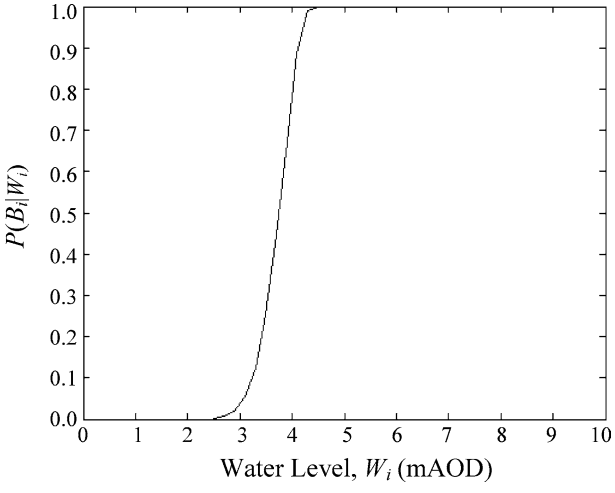

Fig. 1 A fragility function that establishes the relationship between water level and dyke failure probability

dike section i. However, sometimes it may be useful to express the fragility in terms of a function of water level and other variables such as rate of overflow or piping flow rate.

A fragility function may be used to describe multiple and interacting mechanisms of dike response. The example application in this paper includes fragility functions for wall instability, piping and dike crest/rearslope erosion. More comprehensive discussion of dike response to hydraulic loading can be found in Pilarczyk (1998), USACE (2002), Dawson (2003) and HR Wallingford (2004a).

If the water level, W_i, at each dike in the system is a deterministic function of the discharge Q at the upstream boundary of the system, and, furthermore the failure probability of dike sections is independent, conditional upon the loading, then the conditional probability of one of more dike failures in the system, $P(S_s|Q)$ is:

$$P(S_s|Q) = 1 - \prod_{i=1}^{n}[1 - P(B_i|Q)]. \quad (3)$$

The value of Q at which $P(S_s|Q)f(Q)$ is maximised is the 'design point' of the dike system. The probability of any of the 2^n system states can be calculated using the same approach. So, for example the probability of a state S_d (note that the subscript s denotes system failure (i.e. any combination of defence failure), whilst the subscript d denotes a specific combination of defence failure) corresponding to the event $B_1 \cap \ldots \cap B_d \cap \overline{B_{d+1}} \cap \ldots \cap \overline{B_n}$ occurring in load Q is given by:

$$P(S_d|Q) = \prod_{i=1}^{d} P(B_i) \prod_{i=d+1}^{n} [1 - P(B_i)], \quad (4)$$

Fast inundation modelling

Numerical models of floodplain flow range in complexity from fully three-dimensional solutions of the Navier–Stokes equations (Cugier and Le Hir 2002) to models that treat flow as one-dimensional in the down-valley direction. Simulation of inundation over low-gradient floodplains with significant dike structures requires at least a two-dimensional modelling approach with relatively high spatial resolution to represent the complex geometry of the floodplain. However, full two or three-dimensional modelling remains computationally prohibitive on a broad scale if multiple scenarios are to be modelled. The risk assessment methodology presented in this paper is not dependent on the use of a particular inundation model, the only requirement being that the model can resolve the effect of flood dikes and generate a realistic spatial distribution of flood depths within the floodplain. However, to reduce the computational burden of the hydrodynamic calculations for this study a simple two-dimensional raster based inundation model called LISFLOOD-FP was selected. Bates and De Roo (2000) describe the model in detail, however a number of key points are reproduced here. The river channel flow is modelled using the one-dimensional linear kinematic Saint-Venant equations (eg. Chow et al. 1988). When the river channel reaches the top of the dikes, or bankful depth if no dikes exist, flood inundation commences. Flow over dikes is described by standard weir equations (eg. Chadwick and Morfett 1993). Flood wave propagation is represented as an approximation to a two-dimensional diffusive wave. The floodplain is discretised as a grid of rectangular cells. Flow between cells is calculated simply as a function of the free surface height difference across each cell face:

$$Q = \frac{h^{5/3}}{n}\left(\frac{h^{i-1,j} - h^{i,j}}{\Delta x}\right)^{1/2} \Delta y. \quad (5)$$

Change in water depth in a cell over time t_s is calculated by summing the fluxes over the four cell faces.

$$\frac{\mathrm{d}h^{i,j}}{\mathrm{d}t_s} = \frac{Q_x^{i-1,j} - Q_x^{i,j} + Q_y^{i,j-1} - Q_y^{i,j}}{\Delta x \Delta y}, \quad (6)$$

where $h^{i,j}$ is the water free surface height in cell (i,j), Δx and Δy are the cell dimensions, n is a friction coefficient, and Q_x and Q_y describe the volumetric flow rates between floodplain cells. These equations give similar results to a more accurate finite difference discretisation of the diffusive wave equation but with much reduced computational cost, and have been shown to perform as well as full two-dimensional codes (Horritt and Bates 2001) when validated against single synoptic maps of inundation extent.

Numerical method

The main elements of the flood risk analysis method have now been outlined. These are integrated in the methodology summarised in Fig. 2, providing a practical method for solution of Eq. 1. The notable features of the method are the steps that are taken to reduce the computational expense to manageable proportions.

An evenly spaced sample of t points ($t \approx 10$) over the range of Q that has a non-negligible density $f(Q)$ are selected (Fig. 3a). For each point in this sample the hydrodynamic model (with no dike breaches) is run from which the water level, W_i, beside each dike in the system is extracted. In other words, the hydrodynamic model is used to construct a deterministic function $W_i = g_i(Q)$. The fragility function describing the conditional probability of dike breaching given load $P(B_i|W_i)$ is combined with the relation $W_i = g_i(Q)$ to establish the breach probability conditional on flow rate, $P(B_i|Q)$, for each dike section. The conditional probability $P(S_j|Q)$, $j = 1,\ldots,2^n$ of all of the dike system states is calculated using Eq. 4 so that the r system states that make a non-negligible contribution to the total probability $\sum_{j=1}^{2^n} P(S_j|Q) = 1$ (generally $r \lll$

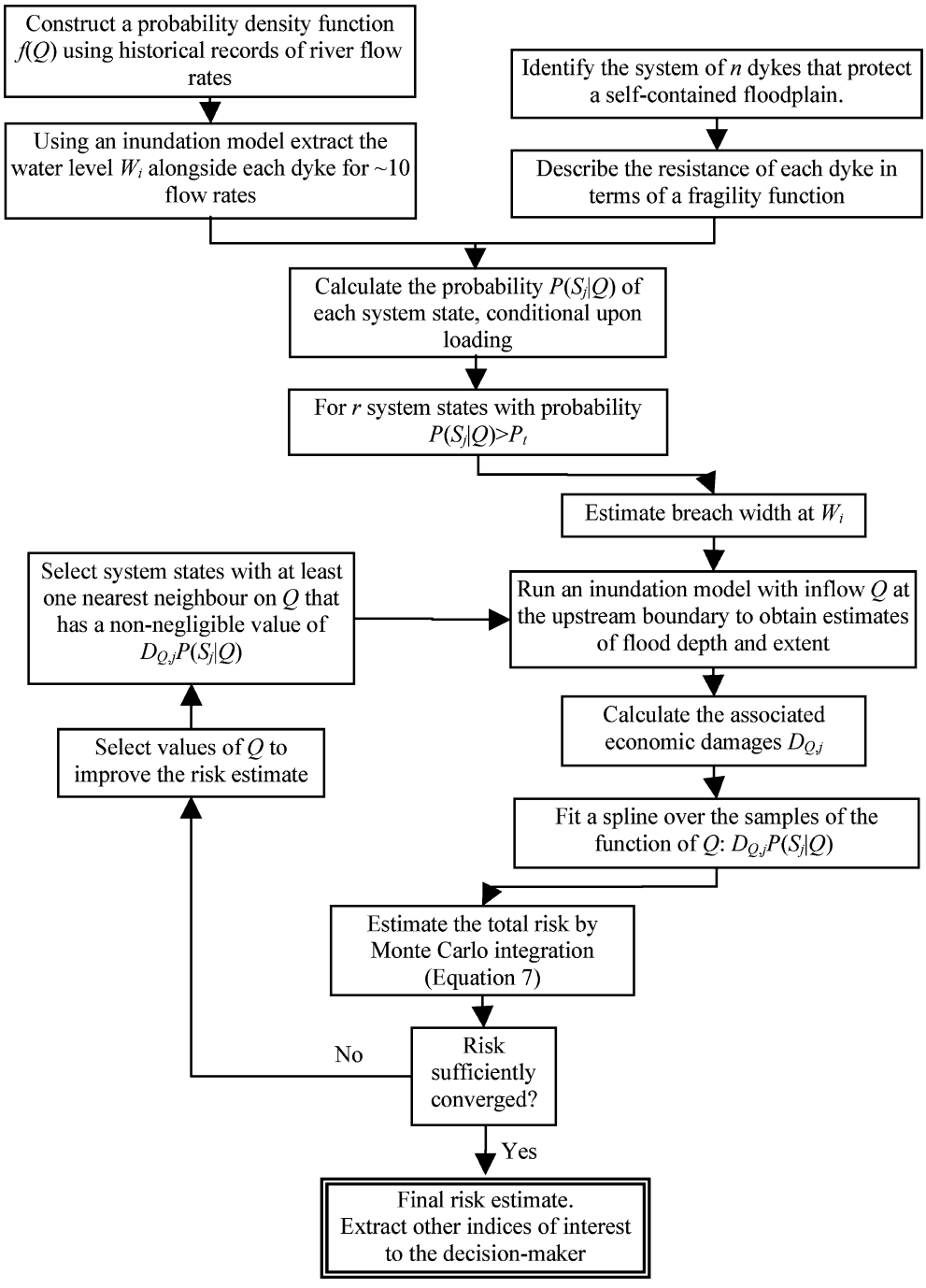

Fig. 2 Overview of risk-based sampling methodology

2^n) are identified. We define a threshold probability P_t below which system states are not tested in the hydrodynamic model. For example, defining $P_t = 0.0001$ meant that for the system presented later in this paper, where $2^n \approx 10^9$, r is a manageable 110 for $Q = 354$ m^3/s, and $\sum_{j=1}^{110} P(S_j|Q) > 0.99$, whilst $\sum_{j=1}^{8} P(S_j|Q) > 0.90$, where the system states are ranked in descending order of $P(S_j|Q)$ (Fig. 3b).

For each of the initial samples of Q and for r system states (labelled S_j: $j = 1,...,r$), the following steps are implemented (note that the first two steps will already have been completed for the dike system state S_1 in which there are no breaches):

1. Modify the dike geometry in the inundation model to represent the dike system state S_j, using an empirical estimate of the breach size and discharge with an incident water level W_i (HR Wallingford 2004b).
2. Run the inundation model using the selected value of Q at the upstream boundary.

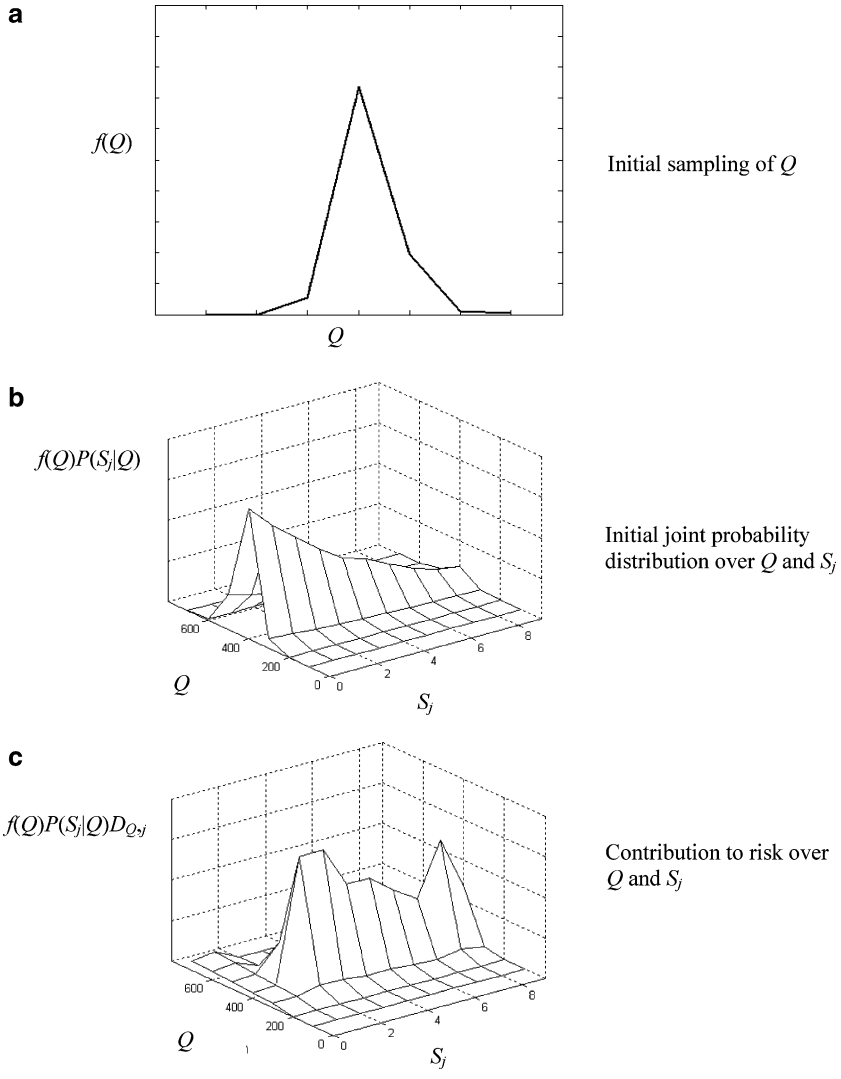

Fig. 3 Steps in the risk analysis (note: $j=0,\ldots,2^{33}$, but only $j=0,\ldots,9$ shown for clarity)

3. For each inundation model run estimate the economic damage, $D_{Q,k}$, using a database of house locations and standard depth-damage criteria (Penning-Rowsell et al. 2003)

Thus for each sample of Q there are r estimates of damage, each one corresponding to a different system state, and for any given system state there are up to t initial estimates of damage, corresponding to different values of Q. For each system state a spline is fitted over the values $D_{Q,j}P(S_j|Q)$, so that at any value of Q an estimate $D_{Q,j}P(S_j|Q)$ can be returned (Fig. 3c) and compared against $P(S_j|Q)$ (Fig. 3b). The integral in Eq. 1 can now be estimated by Monte Carlo integration with m samples from $f(Q)$ so the first estimate $\hat{R}$ of the risk is given by:

$$\hat{R} = \frac{1}{m}\sum_{j=1}^{m}\sum_{k=1}^{r} D_{Q,j}P(S_j|Q_k). \tag{7}$$

This estimate can be improved upon by computing, using the hydrodynamic model, values of $D_{Q,k}$ at more samples points of Q and S_j. A plot of the risk estimate conditional upon Q, i.e.

$$\hat{R}(Q) = \sum_{j=1}^{r} D_{Q,j}P(S_j|Q) \tag{8}$$

gives an indication of the values of Q that contribute most to risk and where more samples of Q are required in order to improve the risk estimate. At each new sampled point of Q we now pre-select the system states to be tested in the inundation modelling, by testing only those states for which, at the nearest lower and upper neighbouring values of Q_k: $k=1,\ldots,t$, tested in the initial analysis, the quantity $D_{Q,j}P(S_j|Q)$ made a non-negligible contribution to the conditional risk estimate $\hat{R}(Q)$. This process relies upon the initial sampling being sufficiently fine to include at least one non-negligible point from each contributing system state. This is achieved by setting the initial threshold probability P_t at a sufficiently low value. System states that make a negligible contribution to risk will be rejected from subsequent analysis.

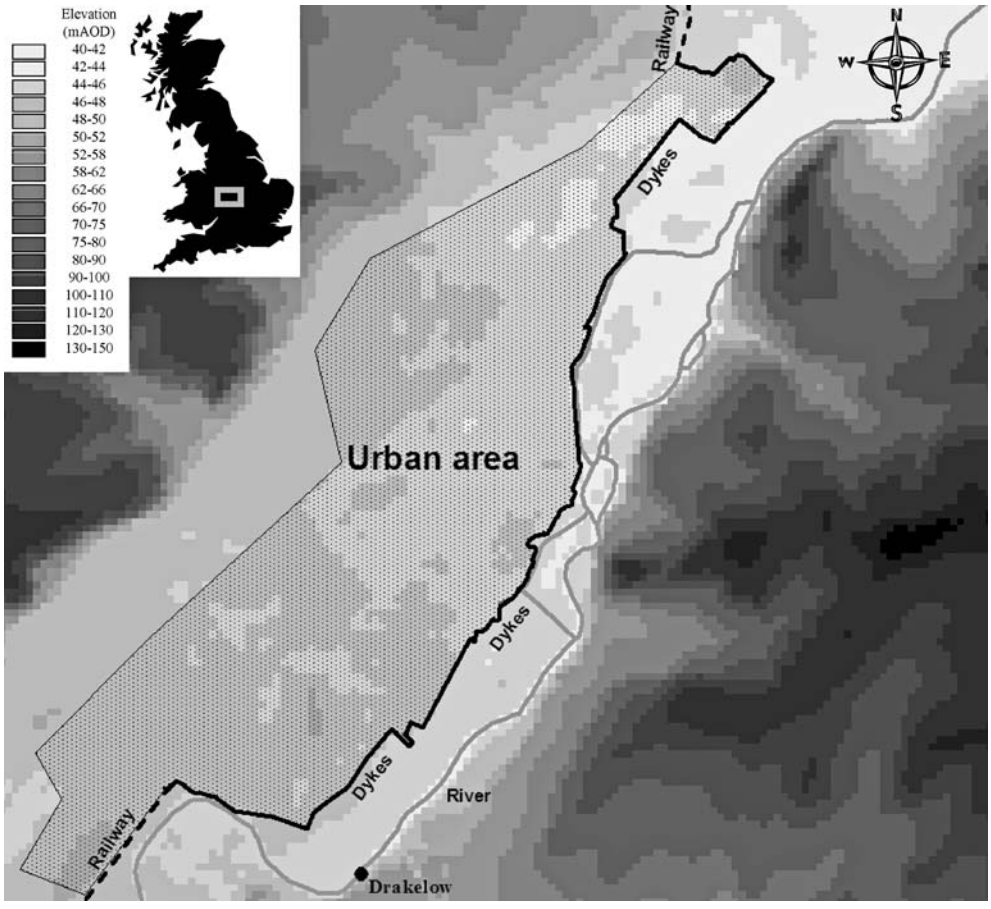

Fig. 4 Maps showing the location of Burton in the UK inset on a DEM of the floodplain (darker shades imply higher ground, scale in mAOD)

The process of estimating $\hat{R}$ and updating the sampling distribution is repeated until the risk has stabilised satisfactorily (Fig. 2).

Example implementation

Background

The case study site selected is the city of Burton-upon-Trent in the UK (Fig. 4). Approximately 10 km of flood dikes protect 12,100 properties of which 10,600 are residential. Only the West side of the river is prone to flooding due to a sharply rising valley on the East side. Most of the dike network is set back from the main river channel(s) meaning many dikes are often unloaded for significant periods of time. Burton has not flooded in recent years, but flow data is available from Drakelow gauging station and water levels alongside the dikes have been recorded for recent high flows in the river. A digital elevation model (DEM) with an r.m.s.e. of ± 1 m was constructed from interferometric synthetic aperture radar (IFSAR) data (Colemand and Mercer 2002).

The dike system

The town is defended by a large network of flood dikes and flanked by raised railway embankments (Fig. 4) at either end of the system. Most of the embankments are sufficiently high to prevent overflow in the 1 in 200 year river discharge. Some are high enough to hold back the water level of the 1 in 1,000 year river discharge. A study of the dike system identified 33 distinct dike sections, the structural integrity of which is good. For each section a dominant mode of failure has been identified, and listed in Table 1. It is worth noting that the number of possible system states is therefore 2^{33} ($\approx$9billion).

Wall instability

The factor of safety (FoS) against wall failure by sliding is defined using (Craig 1992):

$$FoS = \frac{(F_v \tan \varphi + F_p)}{F_a}, \tag{9}$$

where FoS is the factor of safety, F_v is the vertical force, ϕ is the angle of friction between the wall base and the underlying soil, and F_p and F_a are the passive and active forces, respectively in the direction of the river.

The FoS for rotational failure is defined as the ratio of passive and active moment(s) about a point of rotation (Craig 1992):

Table 1 Description of dyke system and their dominant breaching modes

ID	Description	Failure mode
	Railway (South West of modelling domain)	N/A
1	Embankment	Erosion of landward slope due to overflow
2	Embankment	Erosion of landward slope due to overflow
3	Embankment	Erosion of landward slope due to overflow
4	Embankment	Erosion of landward slope due to overflow
5	Embankment	Erosion of landward slope due to overflow
6	Embankment	Erosion of landward slope due to overflow
7	Brick wall	Instability–sliding
8	Embankment	Erosion of landward slope due to overflow
9	Floodbank (embankment with wall)	Instability–overturning or sliding of wall or erosion due to overflow
10	Wall	Instability–overturning or sliding
11	Brick wall	Instability–overturning or sliding
12	Concrete wall	Instability–overturning or sliding
13	Wall	Instability–overturning or sliding
14	Reinforced concrete brick clad wall	Instability–overturning or sliding
15	Masonry wall	Instability–overturning or sliding
16	Brick wall	Instability–overturning or sliding
17	Brick and masonry wall	Instability–overturning or sliding
18	Wall	Instability–overturning or sliding
19	Masonry wall	Instability–overturning or sliding
20	Floodbank	Instability–overturning or sliding of wall or erosion due to overflow
21	Embankment	Erosion of landward slope due to overflow
22	Wall	Instability
23	Embankment	Erosion of landward slope due to overflow
24	Embankment	Erosion of landward slope due to overflow
25	Embankment	Erosion of landward slope due to overflow
26	Floodbank	Erosion of landward slope due to overflow
27	Embankment	Erosion of landward slope due to overflow
28	Brick wall	Erosion of landward slope due to overflow
29	Brick wall	Instability–overturning or sliding
30	Brick wall	Instability–overturning or sliding
31	Embankment	Erosion of landward slope due to overflow
32	Embankment	Erosion of landward slope due to overflow
33	Embankment	Erosion of landward slope due to overflow
	Road (North East of modelling domain)	N/A

N/A not available

$$FoS = \frac{F_p M_p}{F_a M_a}, \tag{10}$$

where M_p and M_a are the moment arms of the passive and active forces, respectively.

The FoS in both cases is used as the basis for assigning failure probabilities. An FoS < 1 implies the system has failed. However, the geotechnical properties of a dike are not spatially homogeneous and the FoS estimate will not be completely certain unless the parameters are exactly known at all points in the dike. The uncertainty representing geotechnical parameters can be described in terms of a probability distribution that captures their spatial variability. The degree of uncertainty associated with the variability is a function of the density of field tests on the dike. Previous borehole investigations had been approximately every 750 m. The cohesion ranged between 0–108 kN/m^2 and the angle of friction $\phi' = 30$–$43°$. Harr (1995) suggests a coefficient of variation for the cohesion, $V_c = 0.4$ and the coefficient of variation for the angle of friction $V_\phi = 0.07$ for gravel soils and $V_\phi = 0.12$ for sandy soils.

Erosion of crest and landward side of embankments

Damage is caused to the crest and landward side of embankments when water is overflowing. Sets of curves established by Bettess and Reeve (1995) indicate the amount of overflow, in terms of head over the embankment crest level, tolerated before damage is likely to occur. The head value is extracted from the hydrodynamic model. The maximum head before damage occurs is dependent on the slope of the landward embankment and the quality and type of protection. Embankments in Burton's dike system are all grass covered.

Piping

None of the dikes at Burton-upon-Trent have been identified as being susceptible to piping failure. However, this is a common failure mode for embankments and has therefore been considered. Stability against piping is established using the formula developed by Terzaghi et al. (1996):

$$C_w = \frac{B/3 + \sum t}{H}, \quad (11)$$

where C_w is the weighted creep ratio which is based on the type of embankment material, B the width of the structure, t the depth of impervious layers below the embankment and H is the pressure head difference across the embankment. Failure probabilities are assigned based on the ratio C_w/C_{wr} where C_{wr} is the critical weighted creep ratio and dependent on the soil type.

Dike breach location and growth

Prediction of dike breach location, geometry and growth rate is highly uncertain. A number of breach models have been developed; these are predominantly parametric or physical process based. For even the most sophisticated models currently available, the uncertainty bounds associated with an estimate of the breach properties are often greater than one order of magnitude (Wahl 1998). Many models are time-dependent in that they attempt to predict breach growth rates, and whilst the risk assessment methodology does not preclude their use, it was considered undesirable to add further computational burden to the inundation modelling process by adding time varying boundary conditions at the dike. A simple parametric relationship was therefore adopted in which the breach width and depth were assumed to remain constant for the duration of the flood event. The dike is assumed to breach to the level of the natural terrain. All breaches are assumed to be centred in the middle of the dike section. A number of simplified rules for breach width have been proposed, including:

$$B = \min\{10h.a, L\}, \quad (12)$$

where h is the head of water, L is the length of the dike section and a is as little as 3 for cohesive materials (HR Wallingford 2004b) and as great as 15 for non-cohesive materials (Visser 1998). For this implementation $a = 6$.

Flow modelling

Thirty-eight years of annual maximum flows recorded at the Drakelow flow gauge from 1962 to 2000, were used to fit the distribution $f(Q)$. Amongst several tested, ln $Q \sim N(170,44)$ fitted the data best (with Q in m^3/s). A design inflow hydrograph had been established by Black and Veatch (2003) using the method proposed by Archer et al. (2000). Information on the river channel dimensions and slope were provided by Black and Veatch (2003). For each simulation the design hydrograph was scaled by the appropriate peak flow rate Q and input as time varying boundary conditions into the hydrodynamic model LISFLOOD-FP at the South-West corner of the model.

The river channel model was calibrated against the 'near-miss' event of November 2000 which provided measured spot heights along the dike system and other minor events that provided in-channel verification of water levels for known events (Black and Veatch 2002). The model was calibrated using the river channel friction, $n_c = 0.03$. The floodplain friction, n_f, chosen was 0.045 to correspond with the values chosen in previous

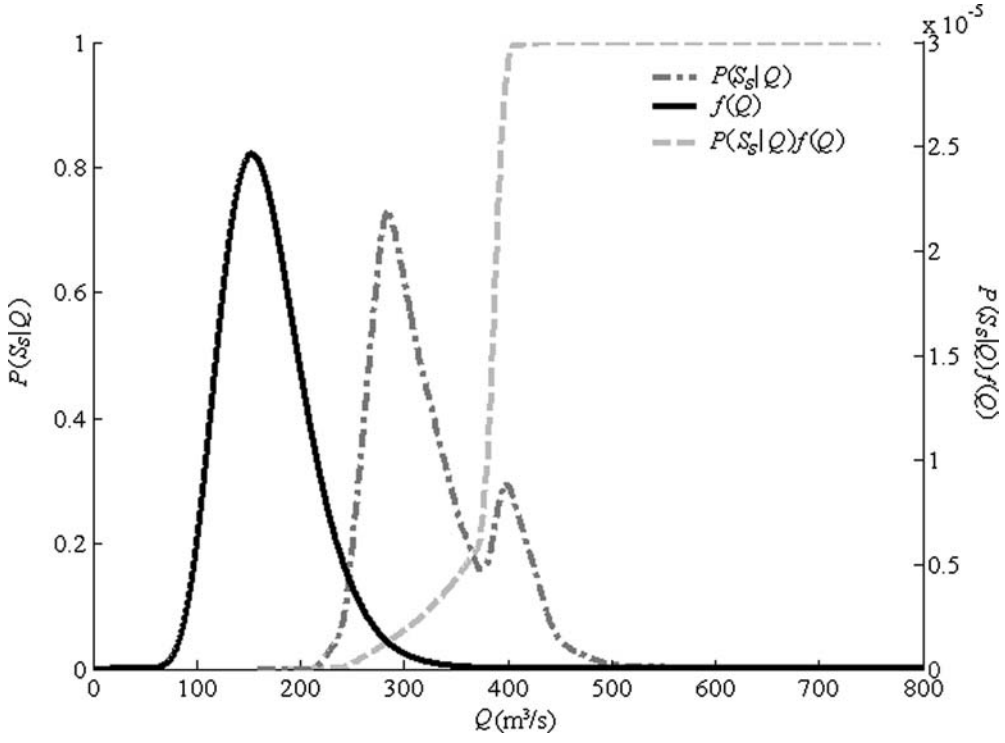

Fig. 5 Plot of $P(S_s|Q)$ (*left axis*) and $P(S_s|Q)\,f(Q)$ (*right axis*) and $f(Q)$ (not plotted to scale)

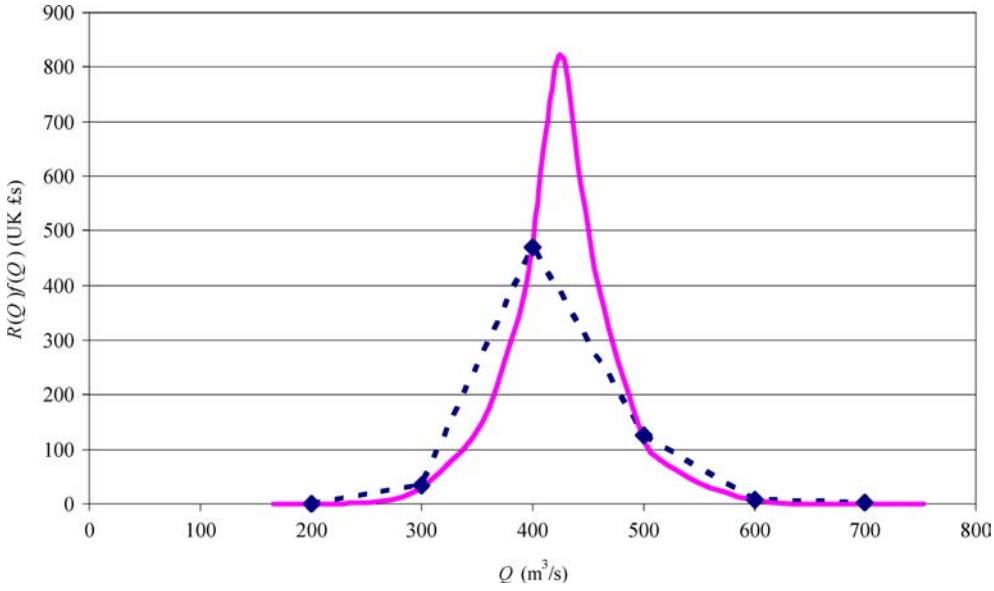

Fig. 6 Plot of flood risk contribution as a function of flow rate (*solid line*) and the points used to construct the initial exploratory risk analysis (*dashed line*)

studies (Black and Veatch 2003) though work by Aronica et al. (2002) and Hall et al. (2005) have shown that the LISFLOOD-FP model is not highly sensitive to floodplain friction parameterization. The modelled water level errors were within ±0.5 m of the measured level.

Implementation of the risk assessment methodology

The conditional probability of systems failure, $P(S_s|Q)$ rises gently between $Q = 250$–375 m^3/s and sharply between $Q = 375$–450 m^3/s (~1:450 year event). This dramatic rise in the systems failure probability, shown in Fig. 5, is predominantly caused by vertical wall instability; as the water level nears the maximum for a given failure mode (eg. rotation) the stability of the wall falls rapidly.

Figure 5 compares three plots, the systems failure probability conditional on flow rate, $P(S_s|Q)$, the p.d.f. describing the flow rate $f(Q)$ and the curve $P(S_s|Q)f(Q)$. The greatest density of $P(S_s|Q)f(Q)$ is at $Q \approx 300$ m^3/s. This part of the curve is dominated by the effect of $f(Q)$, which is also the case for higher flow rates ($Q > 500$ m^3/s). However at $Q \approx 400$ m^3/s the curve $P(S_s|Q)\,f(Q)$ has a secondary-peak caused by interaction between the two components $P(S_s|Q)$ and $f(Q)$.

$\hat{R}(Q)$ is plotted in Fig. 6 and its maximum is at Q≈425 m^3/s. Figure 6 also compares the converged shape of $\hat{R}(Q)$ and the initial estimate $\hat{R}(Q)$ after 6

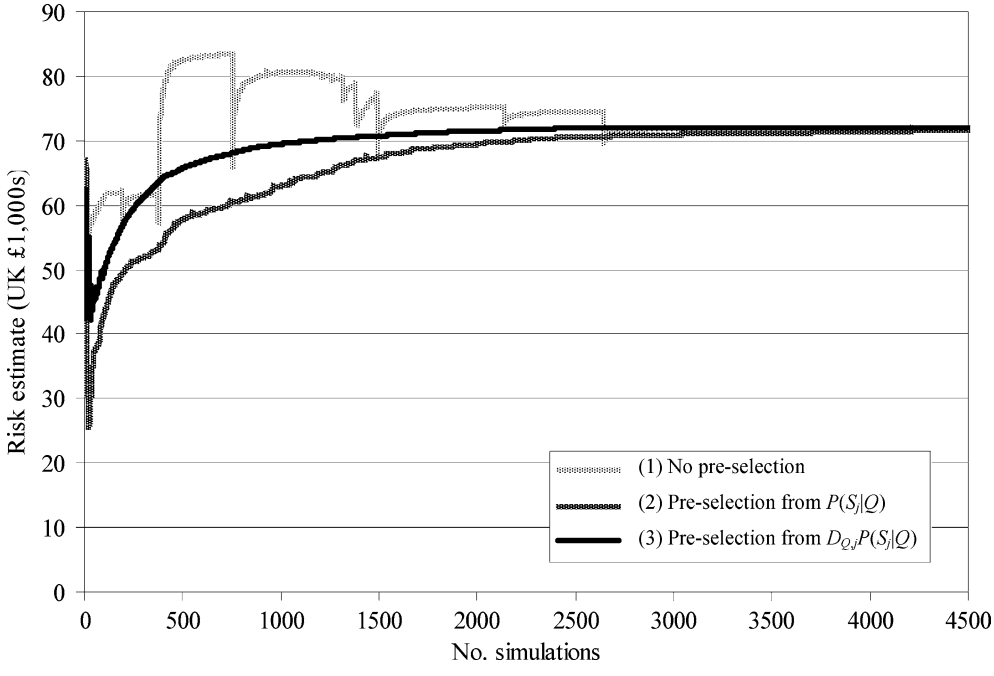

Fig. 7 The convergence of the risk estimator for three different sampling strategies

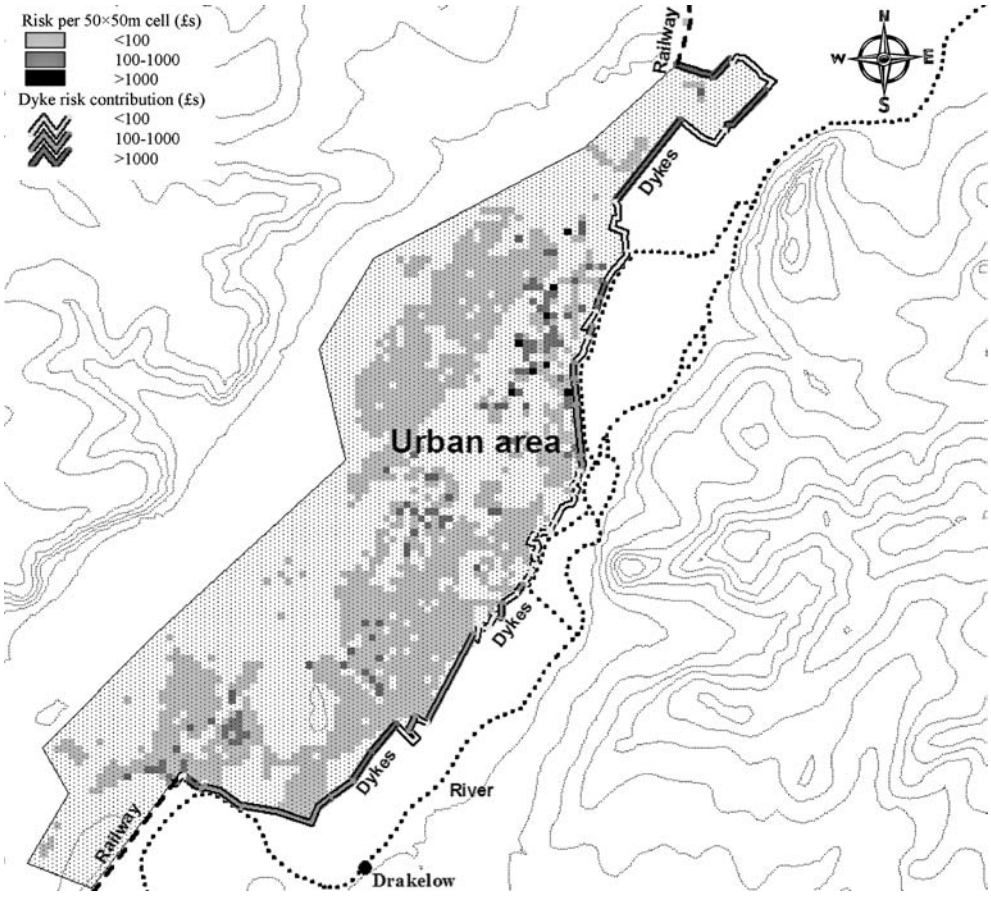

Fig. 8 Spatial distribution of flood risk in the Burton-upon-Trent floodplain and contribution of each dyke to this flood risk (*darker shades* indicate greater flood risk), the valley topography is described by contours

exploratory samples from Q. The present total flood risk, R_{tot}, in terms of expected annual economic damage is £72,000 which is significantly less than the total possible floodplain damage of £1.9billion (estimated by summing, for all properties, the maximum possible damage from the depth-damage curve associated with each property). This low EAD can be attributed to the presence of a dike system that is both in good condition and with crest levels sufficiently high to protect against overflow from events with a return period of 200–1,000 years.

To test the convergence of the sampling method over 5,000 model runs were simulated taking roughly 140 h on a 2.5 GHz PC. The rate of convergence on a final value for EAD is shown in Fig. 7. Three alternative sampling strategies are shown:

1. sampling from $f(Q)$ without pre-selection of the system failure states;
2. sampling from $f(Q)$ with pre-selection of the system failure states on the basis of the probability $P(S_j|Q)$;
3. the method proposed here, where, following an initial exploratory analysis, samples from $f(Q)$ with system states selected on the basis of estimated risk $D_{Q,j}P(S_j|Q)$. The fastest convergence is achieved in the proposed risk-based sampling routine because it optimises the sampling over what is already known about the risk space, whilst the other sampling strategies are aimed at estimating the probability of flooding but not the risk. However, all three sampling strategies converge to within 99% of the final estimate of $\hat{R}$ within 3,000 inundation simulations. This is a marked reduction from the nearly 10^{10} possible simulations for each sample of $f(Q)$. A further attractive property of methods 2 and 3 is that, in this case, the convergence is quite smooth.

In addition to the total risk, other information is readily extracted from the analysis:

(a) spatial distribution of flood risk in the floodplain (Fig. 8),
(b) spatial distribution of inundation probability in the floodplain (Fig. 9),
(c) risk contribution from individual dike sections (Figs. 8, 10),
(d) expected annual damage associated with a given flow rate, water level or return period (eg. $R(Q=354)=$£147 and $R(Q \leq 354)=$£5,454, where $Q=354$ m^3/s is the 1 in 100 year event),
(e) number of properties at risk of flooding to a given depth for a given probability (eg. in Burton 370 properties have a probability of 0.005 that they will be flooded to a depth of up to 0.5 m).

Whilst these outputs provide only a snapshot of the performance and vulnerabilities of the system at pres-

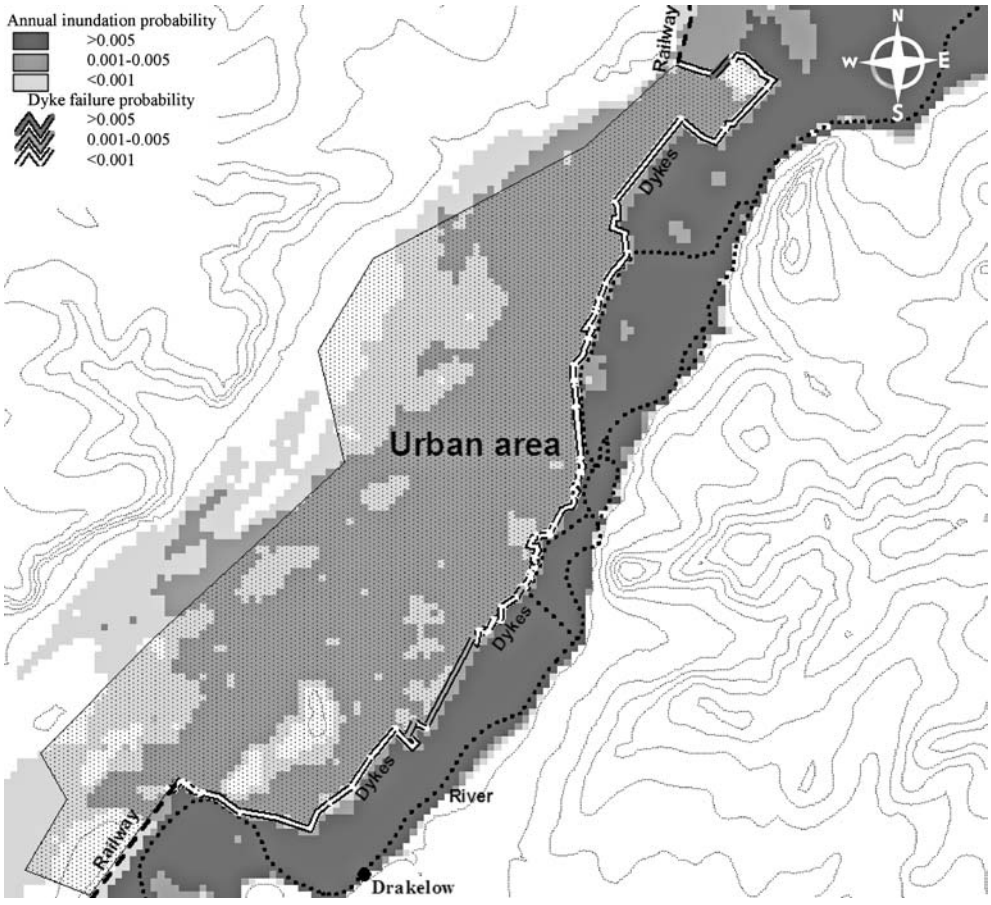

Fig. 9 Spatial distribution of annual inundation probability (*darker shades* indicate greater probability of flooding) and dyke failure probability (*darker shades* indicate greater probability of failure), the valley topography is described by contours

ent, designers and planners may be interested in how future changes to the system (either induced by human or natural causes) may alter this performance in future. The impacts of the construction, maintenance or degradation of infrastructure can be explored by altering the fragility function assigned to the flood dikes and/or the specification of the hydrodynamic model before re-running the sampling routine. Socio-economic changes, such as housing or industrial development or abandonment can be explored through alteration of the database of domestic or commercial properties. Non-structural mitigation measures such as flood warning, flood resistant development and public education can be modelled through changes to the depth-damage relationship.

Changes to the loading regime, perhaps resulting from climate change, can also be considered. DEFRA (2002) suggest that future flood management strategies should be sensitivity tested against a 20% increase in extreme flow rate to consider possible impacts of climate change over the next 50 years. Assuming all other parameters remain constant, in this example, the EAD at year 50 would increase to £1,042,000 (a factor of 14) if this were to occur. This large increase in flood risk is attributable to the presence of the flood defences that causes the system to be fragile.

Figure 8 shows the spatial distribution of flood risk in the floodplain and the contribution towards this risk from each defence. The risk is generally evenly spread over the floodplain with a few localised areas of high risk, usually resulting from high building density. The annual inundation probability behind the dike system, shown in Fig. 9, is less than 0.005 and generally decreases with distance from the structures. Comparing Figs. 8 and 9 it is clear that a large dike failure probability does not always correspond to a higher contribution towards flood risk. Figure 11 shows four flood outlines and their associated damages $D_{Q,j}$ and conditional risk $D_{Q,j}P(S_j|Q)$ for four different system failure states for $Q = 354$ m^3/s. Despite the same load being imposed on the system, the flood outlines and resultant values of $D_{Q,j}$ are very different. A higher $D_{Q,j}$ does not necessarily correspond to the highest risk contribution $D_{Q,j}P(S_j|Q)$. This is caused by a number of factors; the probability of given system state, the loading on the system, the spatial distribution of the floodplain assets, the type of floodplain asset and the floodplain topography. For larger flow rates, system states with more than one breach account for an increasingly significant proportion of the risk. The double dike failure shown in Fig. 11d contributes more towards flood risk than the single defence failures shown (although this is not the case for all double dike failures).

Clearly, larger loads or weaker dikes will increase the flood risk associated with a given dike system. However, where the local topography is such that only small vol-

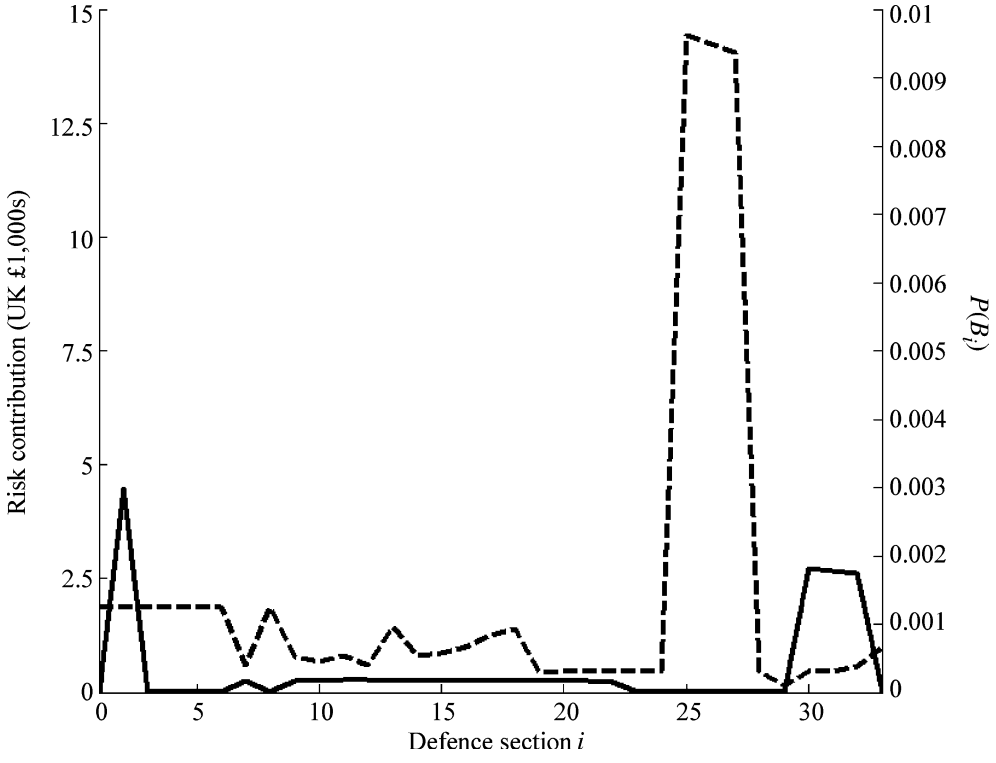

Fig. 10 Failure probability (*solid line*) and contribution towards flood risk (*dashed line*) of each dike section

umes of water can enter the floodplain, the risk is greatly reduced, likewise if the region in close proximity to the location of the dike failure is sparsely populated. These factors are shown in Fig. 11b and d where high flood damages associated with the dike system state because they result in the flooding of numerous non-residential properties (supermarkets, industrial estates etc.). Figure 11c shows how factors such as the dike size and local topographical features surrounding the dike breach can inhibit the volume of water able to flow into the floodplain. The flood extent of Fig. 11a is forced to flow round raised ground to the East of the breach.

A comparison of the four very different values of $D_{Q,j}$ in Fig. 11 justifies the use of a hydrodynamic inundation model. Use of a 'bathtub' model that intersects the DEM with the water level at the breach would provide a conservative estimate of $D_{Q,j}$ and result in significantly larger estimates of flood risk. However, at the highest flow rates, a 'bathtub' model is more acceptable: regardless of the dike system state, the volume of water entering the floodplain is always sufficiently large that the flow is constricted by the West side of the valley.

Despite the greatest density of $P(S_s|Q)\ f(Q)$ (i.e. the system design point) being at $Q \sim 280$ m^3/s the flood risk contribution from these flow rates is negligible. This serves to demonstrate how different the probability and risk contribution can be for a given system state. Whilst the probability contributions are greatest for $Q < 300$ m^3/s, the risk is negligible, and for $R(Q \leq 200) = 0$ because even in the case of a dike breach water is unable to enter the floodplain due to the underlying topography. This is an important observation as systems are often optimised around their design point, which in this case has been shown to be very distant from the region of maximum risk. However, it should be noted that the peak of $R(Q)$, ($Q \approx 425$ m^3/s), is near the secondary maxima, ($Q \approx 400$ m^3/s), on $P(S_s|Q)f(Q)$ shown in Fig. 5. Therefore, whilst other factors influence the risk, the systems failure probability, $P(S_s|Q)f(Q)$, does show some relation to the behaviour of the function $R(Q)$.

Conclusions

An adaptive systems-based risk assessment methodology has been demonstrated that efficiently samples the risk response-surface to reduce the computational burden of analysing every possible system state for the entire loading space. Risk has been shown to be a complex function of loading, dike(s) properties, floodplain topography, the geographical location and type of assets in the floodplain. A limited assessment that considered conditions only at the system design point, or a limited number of dike failure combinations would not, in the UK floodplain considered here, have adequately captured important system behaviour.

The analysis dealt with two uncertainties in probabilistic terms: the flow in the river at the upstream boundary of the hydrodynamic model and the failure of the dike sections in the system. More comprehensive uncertainty analysis would include the uncertainties in

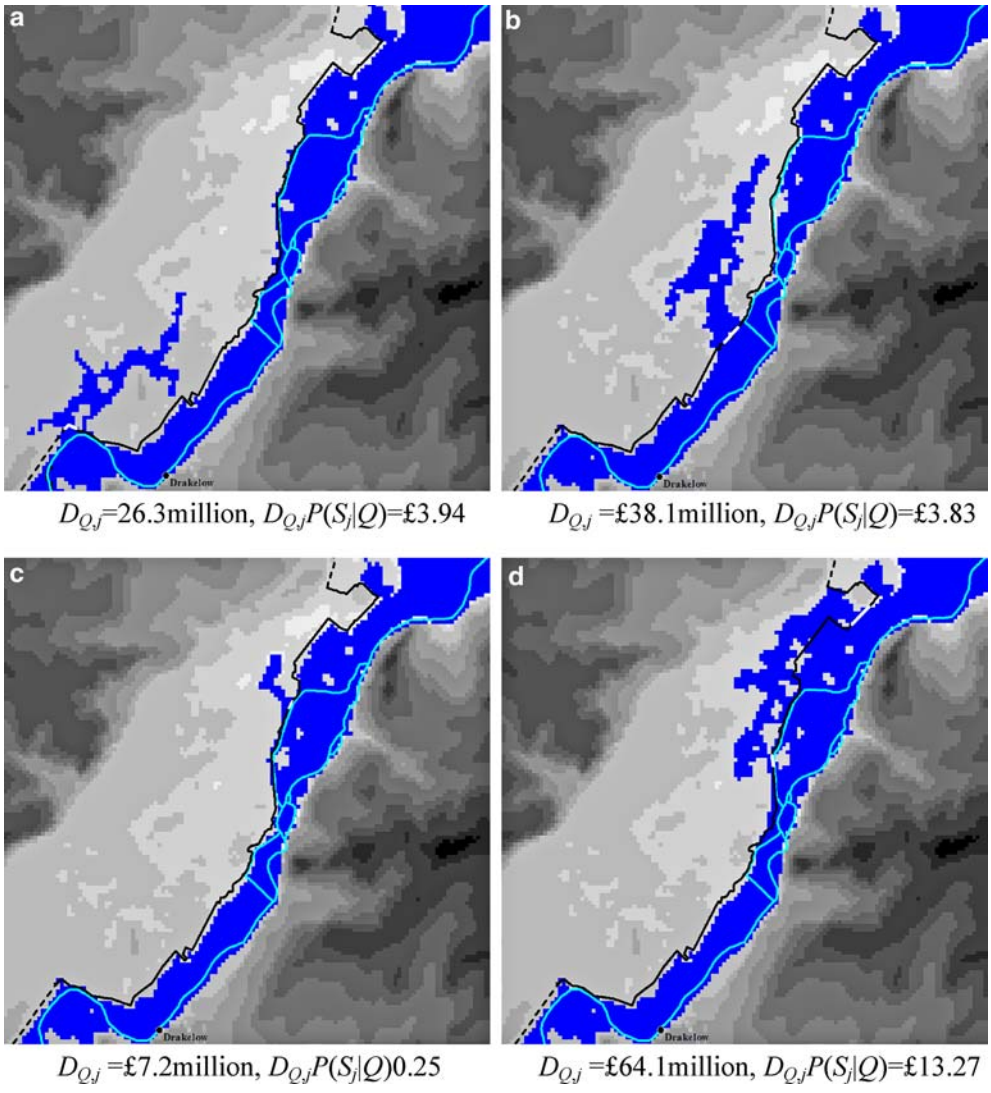

Fig. 11 Four flood outlines for breach scenarios for $Q = 354$ m^3/s (the 1:100 year event), **a**–**c** are single dyke failure scenarios, **d** shows a double dyke failure scenario

the hydrodynamic model of river flow and floodplain inundation [roughness parameterisation, channel dimensions and floodplain elevation (Hall et al. 2005)] and uncertainties in the damage calculation. The reliability analysis could be extended to include more failure modes and spatial dependency in the variables describing dike resistance. Further extensions to more comprehensive risk analysis would include the effects of drainage systems. However, whilst possible, each of these extensions would add computational expense.

The example implementation at Burton-upon-Trent in the UK demonstrates that the methodology provides an efficient means of assessing the flood risk of a complex dike system. The methodology also identifies the contribution to flood risk of individual dike sections as well as a spatial distribution of flood risk and inundation probability in the floodplain, amongst other insights for decision-makers. The methodology can be used to assist catchment managers identify appropriate resource allocation strategies and test scenarios of changed extreme river flow rates, investment in flood dike infrastructure and floodplain occupancy. It can also form the basis for a more detailed analysis and provide feedback to national scale risk assessments.

Acknowledgements The research described in this paper formed part of the ''RASP: Risk assessment for flood and coastal defence systems for strategic planning'' project, funded by the Environment Agency within the joint DEFRA/EA Flood and Coastal Defence R&D programme. Data used in the case study was provided by The Environment Agency and Black and Veatch Ltd. Dr. Rosu was funded by a European Commission Marie-Curie research fellowship.

References

Archer D, Foster M, Faulkner D, Mawdsley J (2000) The synthesis of design flood hydrographs. In: Proc. ICE/CIWEM Conf. Flooding–Risks and Reactions. Terrace Dalton, London

Aronica G, Bates PD, Horritt MS (2002) Assessing the uncertainty in distributed model predictions using observed binary pattern information within GLUE. Hydrol Process 16:2001–2016

Bates PD, De Roo APJ (2000) A simple raster-based model for flood inundation simulation. J Hydrol 236:54–77
Bedford T, Cooke RM (2001) Probabilistic risk analysis: foundations and methods. Cambridge University Press, Cambridge
Bettess R, Reeve CE (1995) Performance of river flood embankments. HR Wallingford Report SR 384
Black and Veatch (2002) Fluvial trent strategy—interim hydrology report. Black and Veatch Ltd
Black and Veatch (2003) Fluvial trent strategy—interim hydraulic modelling report. Black and Veatch Ltd
Bye P, Horner M (1998) Report by the independent review team to the board of the environment agency. Vols 1 and 2, Environment Agency, Bristol
Casciati F, Faravelli L (1991) Fragility analysis of complex structural systems. Research Studies Press, Taunton
Chadwick A, Morfett J (1993) Hydraulics in civil and environmental engineering, 2nd edn. E& FN SPON, London
Chow VT, Maidment DR, Mays LW (1988) Applied hydrology. McGraw-Hill, New York
Colemand MD, Mercer JB (2002) NEXTMap Britain: completing phase 1 of Intermap's global mapping strategy. GeoInformatics December 2002, pp 16–19
Craig RF (1992) Soil mechanics, 5. Chapman and Hall, London
Cugier P, Le Hir P (2002) Development of a 3D hydrodynamic model for coastal ecosystem modelling. Application to the plume of the Seine River (France). Estur Coast Shelf Sci 55(5):673–695
Dawson RJ (2003) Performance-based management of flood defence systems. PhD Thesis, University of Bristol
Dawson RJ, Hall JW (2002a) Improved condition characterisation of coastal defences. In: Proc. of ICE conference on coastlines, structures and breakwaters. Thomas Telford, London, pp 123–134
Dawson RJ, Hall JW (2002b) Probabilistic condition characterisation of coastal structures using imprecise information. In: McKee Smith J (ed) Coastal engineering 2002, Proceedings of the 28th International Conference, Cardiff UK, July 8–12, 2002. New Jersey: World Scientific, vol 2, pp 2348–2359
DEFRA (2002) UK climate impacts programme 2002 climate change scenarios: implementation for flood and coastal defence: guidance for users. R&D Technical Report W5B-029/T. DEFRA, London
Environment Agency (2001) Lessons learned: autumn 2000 floods. Environment Agency, Bristol
Halcrow, HR Wallingford, John Chatterton Associates (2001) National appraisal of assets at risk from flooding and coastal erosion including the effects of climate change. DEFRA, London
Hall JW, Dawson RJ, Sayers P, Rosu C, Chatterton J, Deakin R (2003a) A methodology for national-scale flood risk assessment. J Water Maritime Eng 156(3):235–247
Hall JW, Meadowcroft IC, Sayers PB, Bramley ME (2003b) Integrated flood risk management in England and Wales. Nat Hazard Rev 4(3):126–135
Hall JW, Tarantola S, Bates PD, Horritt MS (2005) Distributed sensitivity analysis of flood inundation model calibration. ASCE J Hydraulic Eng 131(2):117–126
Harr ME (1995) Accounting for variability (reliability). In: Chen WF (ed) The civil engineering handbook. CRC, Boca Raton, pp 683–704
Horritt MS, Bates PD (2001) Predicting floodplain inundation: raster-based modelling versus the finite-element approach. Hydrol Process 15:825–842
ICE (2001) Final report of the ICE's presidential commission to review the technical aspects of flood risk management in England and Wales: learning to live with rivers. Institution of Civil Engineers, London
JCSS–Joint Committee on Structural Safety (1981) General principles on reliability for structural design. Int. Assoc. for Bridge and Structural Engineering
Jonkman SN, Van Gelder PHAJM, Vrijling JK (2003) Flood risk calculated with different risk measures. In: McKee Smith J (ed) Coastal Engineering 2002, Proceedings of the 28th international conference, Cardiff UK, July 8–12, 2002. New Jersey: World Scientific, vol 2, pp 2360–2372
Jorissen RE, Stallen PJM (1998) Quantified societal risk and policy making. Kluwer, Dordrecht
Melchers RE (1999) Structural reliability analysis and prediction, 2nd edn. Wiley, Chichester
Moser DA (1997) The use of risk analysis by the US Army Corps of Engineers. In: Proceedings hydrology and hydraulics workshop on risk-based analysis for flood damage reduction studies. USACE, pp 1–14
NAO (2001) Inland Flood Defence. Report by the comptroller and auditor general of the National Audit Office. HMSO, London
NRC (National Research Council) (2000) Risk analysis and uncertainty in flood damage reduction studies. National Academy Press, Washington DC
Penning-Rowsell EC, Johnson C, Tunstall SM, Tapsell SM, Morris J, Chatterton JB, Coker A, Green C (2003) The benefits of flood and coastal defence: techniques and data for 2003. Middlesex University Flood Hazard Research Centre
Pilarczyk KW (1998) Dykes and revetments: design, maintenance and safety assessment. Balkema, Rotterdam
Sayers PB, Hall JW, Meadowcroft IC (2002) Towards risk-based flood hazard management in the UK. Proceedings of the Institution of Civil Engineers: Civil Engineering, 150(Special Issue 1):36–42
Tapsell SM, Penning-Rowsell EC, Tunstall SM, Wilson TL (2002) Vulnerability to flooding: health and social dimensions. Phil Trans Royal Soc Lond A360:1511–1525
Terzaghi K, Peck RB, Mesri G (1996) Soil mechanics in engineering practice, 3rd edn. Wiley, New York
USACE (1996) Risk-based analysis for flood damage reduction studies. Report EM1110–2-1619, United States Army Corps of Engineers, Washington
USACE (1999) Risk assessment handbook, Volume I: Human health evaluation and risk assessment handbook, Volume II: Environmental evaluation. Engineering manual EM 200–1-4
USACE (2002) Coastal engineering manual. USACE, Manual EM 1110–2-1100 http://www.usace.army.mil/inet/usace-docs/eng-manuals/
Van Gelder PHJM, Vrijling JK (1998) The effect of inherent uncertainty in time and space on the reliability of flood protection. In: Lydersen S, Hansen GK, Sandtorv H (eds) Safety and reliability, Proceedings ESREL '98 Conference, Trondheim, Norway, Balkema, Rotterdam, pp 451–456
Visser PJ (1998) Breach Growth in Sand defences. Communication on Hydraulic and Geotechnical Engineering. TU Delft Report no. 98–1
Voortman HG, Van Gelder PHAJM, Vrijling JK (2003) Risk-based design of large-scale flood defence systems. In: McKee Smith J (ed) Coastal Engineering 2002, Proceedings of the 28th international conference, Cardiff UK, July 8–12, 2002. New Jersey: World Scientific, vol 2, pp 2373–2385
Vrijling JK (2001) Probabilistic design of water defence systems in The Netherlands. Reliabil Eng Syst Saf 74:337–344
Wahl TL (1998) Prediction of embankment dam breach parameters: a literature review and needs assessment. Dams Safety Office: DSO-98–004 http://www.usbr.gov/pmts/hydraulics_lab/twahl/
Wallingford HR (2004a) Performance and Reliability of Flood and Coastal Defences–Phase I: Literature Review, DEFRA/EA R&D Programme R&D Report
Wallingford HR (2004b) Investigation of extreme flood processes& uncertainty (IMPACT) EC Research Project No. EVG1-CT2001–00037- http://www.impact-project.net